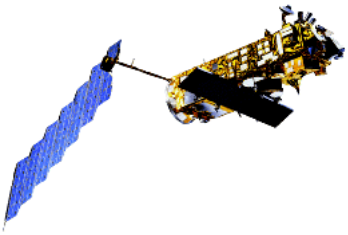

ENVISAT Microwave Radiometer Assessment Report

Cycle 051

04-09-2006 – 09-10-2006

Prepared by :	M. DEDIEU, CETP L. EYMARD, LOCEAN/IPSL E. OBLIGIS, CLS OZ. ZANIFE, CLS F. FERREIRA, CLS	
Checked by :	L. EYMARD, LOCEAN/IPSL	
Approved by :	P. FEMENIAS, ESA	

CLS.DOS/06.230
Edition 1.1, October 2006

Contents

1 Editing modifications 2

2 Introduction 3

3 Maps of the brightness temperatures over South Pole 4

4 Monitoring of the radiometer internal parameters 6

5 Monitoring of cold ocean brightness temperatures 11

6 Conclusion on the cycle assessment and long term monitoring 13

7 Reference documents 14

1 Editing modifications

Version	Date	Object
1.0	June 2002	Creation of the document.
1.1	May 2006	Add monitoring anomalies table (table 1).

2 Introduction

This document aims at reporting the behavior of ENVISAT Microwave Radiometer in terms of instrumental characteristics and quality of the brightness temperatures for cycle 051 (from 04-09-2006 to 09-10-2006) corresponding to day 1648 to day 1683 since ENVISAT launch.
It is performed on the MWR level 0 data product (MWR_NL_OP). The decoding and the pre-processing are done with the MWR level 1B reference processing chain located at CETP. The data are from the ESA's ground stations in Kiruna, Sweden, and at ESRIN, Italy.

The objectives of this document are :

- to provide an instrumental status
- to check the stability of the instrument
- to report any change at the instrumental level likely to impact quality of the brightness temperatures

It is divided into the following topics:

- Maps of the brightness temperatures over South Pole
- Monitoring of the radiometer internal parameters
- Monitoring of cold ocean brightness temperatures
- Conclusion on the cycle assessment and long term monitoring

3 Maps of the brightness temperatures over South Pole

Over poles, the space and time coverages are sufficient to draw maps of the brightness temperatures. Since the atmospheric variability is weak due to the very low water vapour content, the brightness temperatures are mainly representative of surface emissivity and temperature variations, which slowly vary within the course of the year. Consequently, the south pole can be used as a stable target to monitor the brightness temperature variations with time.

Figure 1 (top) and (bottom) show respectively the 23.8 and 36.5 GHz brightness temperatures measured by the radiometer over the South pole (latitudes higher than 65^{o}S) for the current cycle. The ice cap appears colder than the sea ice and the free water at the two frequencies.

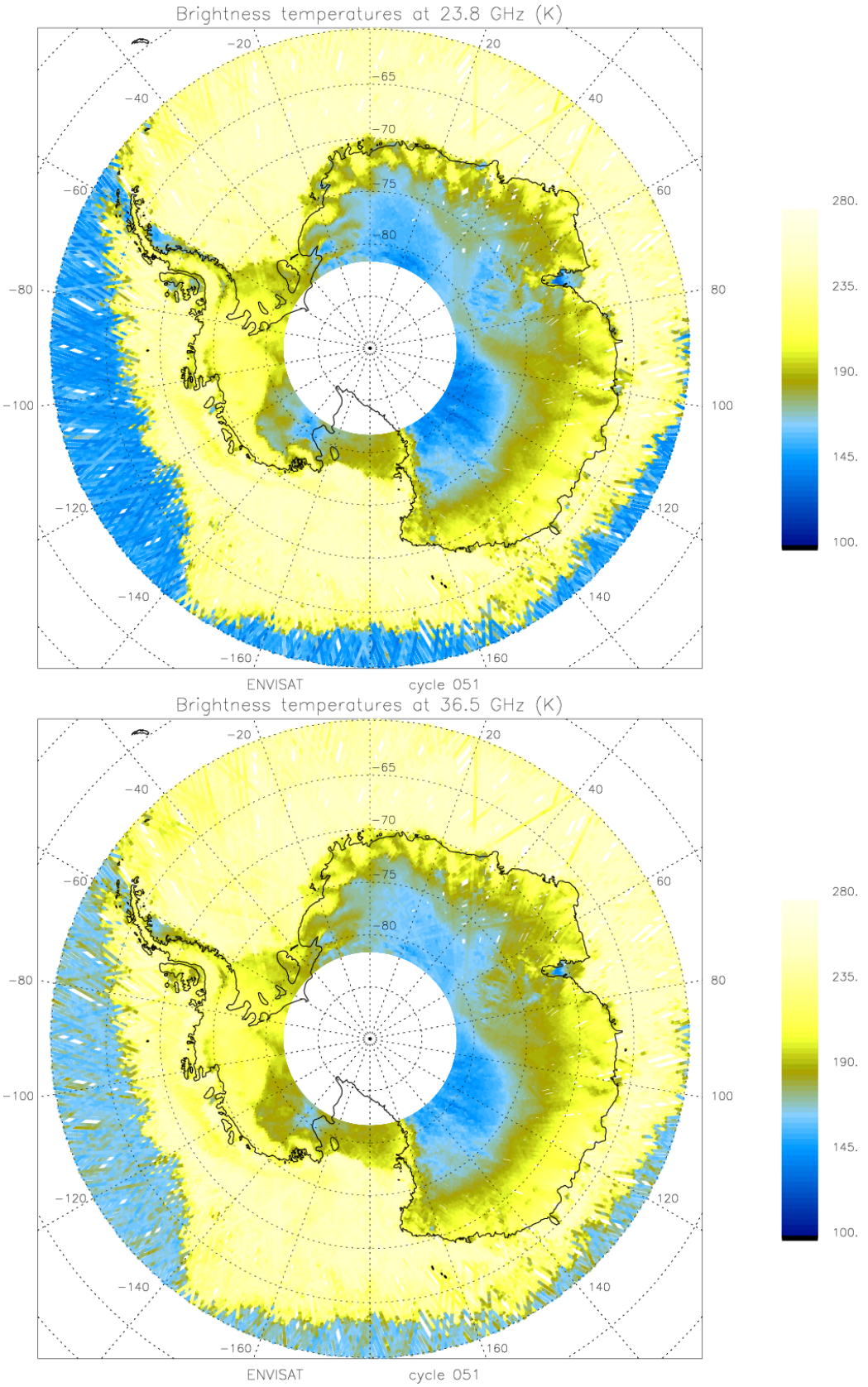

Figure 1: Brightness temperature maps over the South Pole for the two frequencies, 23.8 and 36.5 GHz.

4 Monitoring of the radiometer internal parameters

The radiometer telemetry primarily contains the radiometer counts for each channel, which are related to the brightness temperatures of the main antenna and the two calibration loads, through the working model (Bernard et al, 1993) summarized below:

$$\mathbf{Tfc} = acc\ ah0\ \mathbf{TC} + (1 - acc)\ ah0\ \mathbf{Tcc} + (1 - ah0)\mathbf{Th}$$

$$\mathbf{G} = (Cc - Cf)/[ao + af\ \mathbf{Tfc} - ac\ \mathbf{Tc} + ah\ \mathbf{Th/c}]$$

$$\mathbf{TE} = (Cc - off)/\mathbf{G} - aref\ \mathbf{Tref} - ad\ \mathbf{Td} + a2\ \mathbf{Tfc} + a3\ \mathbf{Th/c} + a4\ \mathbf{Tc} + a6\ \mathbf{Tcal} + a5$$

$$\mathbf{T'a} = b1\ \mathbf{Tref} + b2\ \mathbf{Td} - b3\ \mathbf{Tcal} - b4\ \mathbf{Tc} + \mathbf{TE} - (Ca - off)/\mathbf{G}$$

$$\mathbf{Ta} = c1\ \mathbf{T'a} - c2\ \mathbf{Tr}$$

where the coefficients are derived from the primary coefficients shown in **figure 2**. The brightness temperature is then derived from the antenna measurement, by accounting for the reflector losses and side lobe contributions.

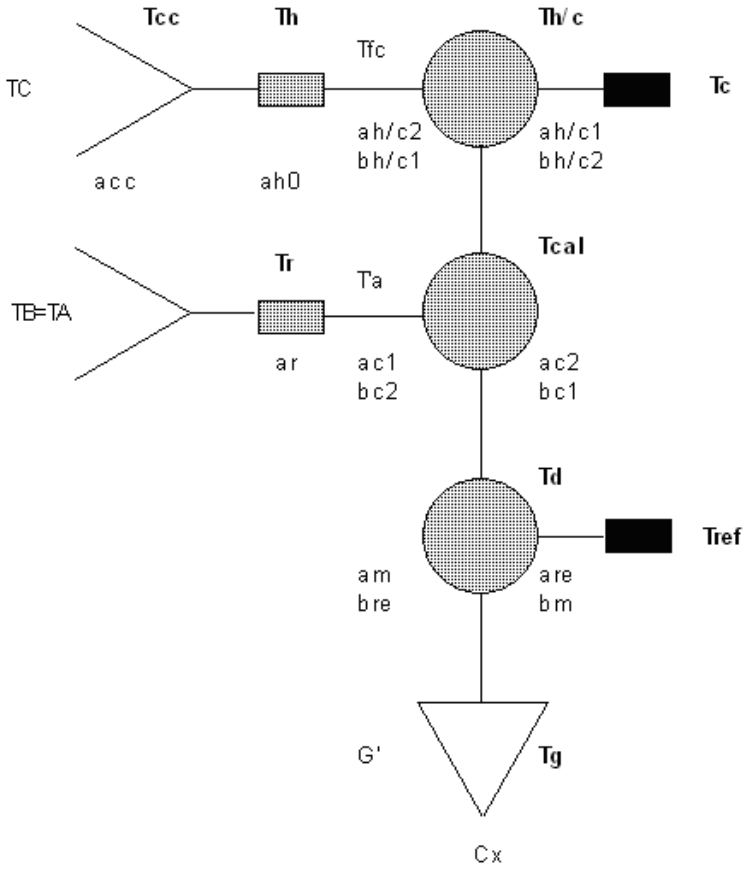

Figure 2: scheme of one channel of the MWR, showing the main antenna, whose measurement is TA, the two calibration loads, consisting of an internal hot load and a sky horn, the reference load (Dicke load - temperature Tref) and internal switches to get every measurement. Each component is characterized by transmission and loss factors which are taken into account in the radiometer model, as well as their temperature.

To monitor the instrument behaviour during its lifetime, the key parameters are plotted in **figures 3 to 5** : gain (after correction of the thermal variations, modeled as a parabolic function), hot load and sky horn counts, and the residual term TE (residual temperature contribution due to errors in the estimated coefficients).
The instrument stability is ensured if none of these parameters do vary with time.

Figure 3 represents the gains of the two channels 23.8 and 36.5 GHz since Envisat launch (top), and on the last 10% of time (bottom). They show that the gain in the 23.8 GHz channel remains stable around 9.6. For the second channel, the evolution shows two decreasing trends, small at the beginning (starting around day 25) and a stronger one since days around 150 after launch. The total decrease is about 19.92% (at 10.4 at the beginning and about 8.328 now).
Note that a step down on the gain values around day 1150 for 36.5 GHz channel and a big spike around day 1433 for both channels are observed.
For cycle 045, a slight jump in the very last days of cycle 045 is observed.
A plateform deficiency has occured from day 1497 to day 1500 from launch (cycle 046). Then, gain loss is observed for both channels on figures. A spike is also observed around day 1505 for both channels.
Note that no level 0 data was available between 7th, September 2006 and 11th, September 2006 first, and second, between 26th, September 2006 and 1st, October 2006. First unavailable period is related to Servive Module Anomaly, while second one refers to interruption of Envisat data transmission via the ESA Data Relay Satellite Artemis. Holes in gain representation (figure 3) are related to these both periods.

The sky horn counts on **figure 4** exhibit similar features than the gain for both channels. The counts present a very slight increase with time for the first channel. For the second one, the values drop from 3600 to 2983 (-17.14%). The hot load counts on the same figure are stable for the first channel, around 553. They decrease for the second channel from 660 at launch time to about 631 (-4.39%).
However, a slight increase of hot load counts is observed in the very last days of cycle 045 for first channel, while, for the second one, the increase is observed since the early days of cycle.
Note that spikes observed between days 1500 and 1505 are related to gain incidents invoked above.

Finally, **figure 5** shows the residual temperature. Since launch, the values are higher than evaluated from ground testing. The residual temperature was expected to be around 0.5 K for the first channel and a bit higher, 0.5-0.7 K for the second one, i.e. close to the ERS ones (Eymard et al, 2002).
Note that a big spike around day 1433 for both channels are observed, as it is on gain values.
Note that a residual temperature increase is observed after this spike for channel 1, during cycle 045.

There are 4 particular features of this parameter to analyse:

- a drift of the residual temperature at 36.5 GHz, the values were down to -2.5 K with a regular linear decrease since 2-3 months after launch to days around $\sim$450.
- a step is then observed with an increase of 0.5 K. The values were around -2.0 K and are decreasing again and are around -3.60 K.
- a step is observed at 23.8 GHz around day 260 with an increase of 0.5 K.
- a decrease is observed after the previous mentionned step for the 23.8 GHz channel. Since day 450 the values vary around 1.

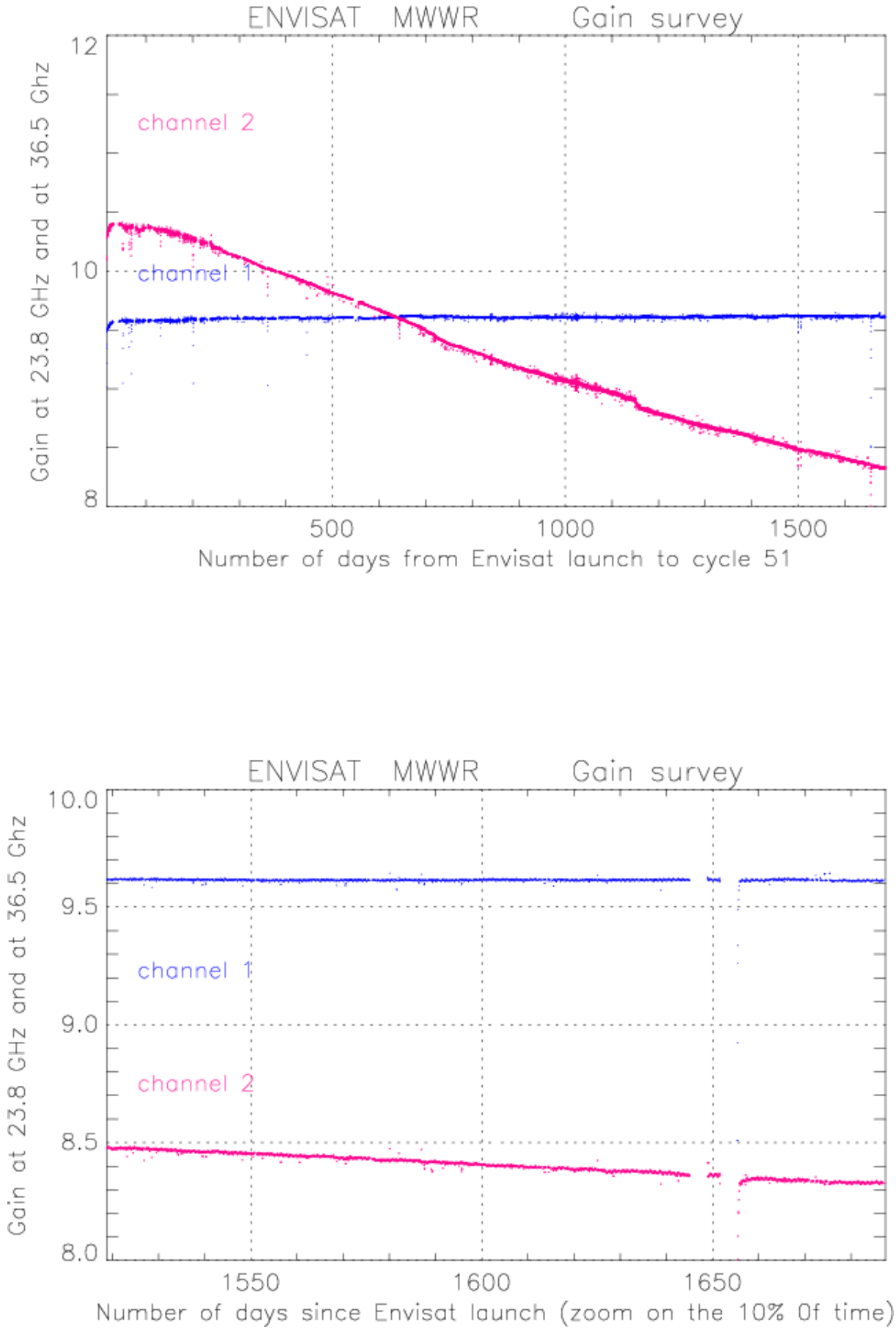

Figure 3: Time evolution of the gain since Envisat launch (March 1st, 2002 - data available since March 15th).

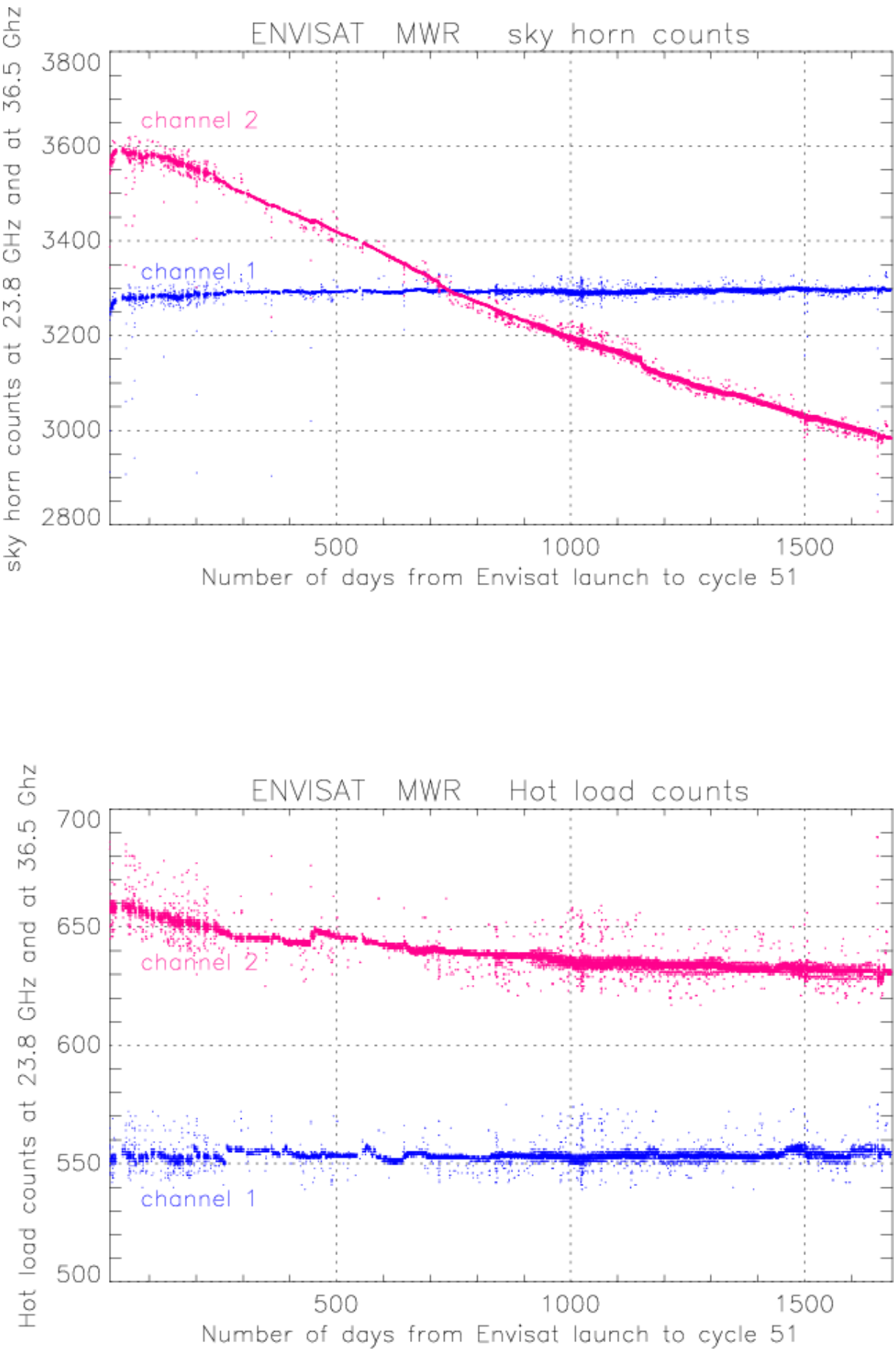

Figure 4: Time evolution of the sky horn count and the hot load count since Envisat launch.

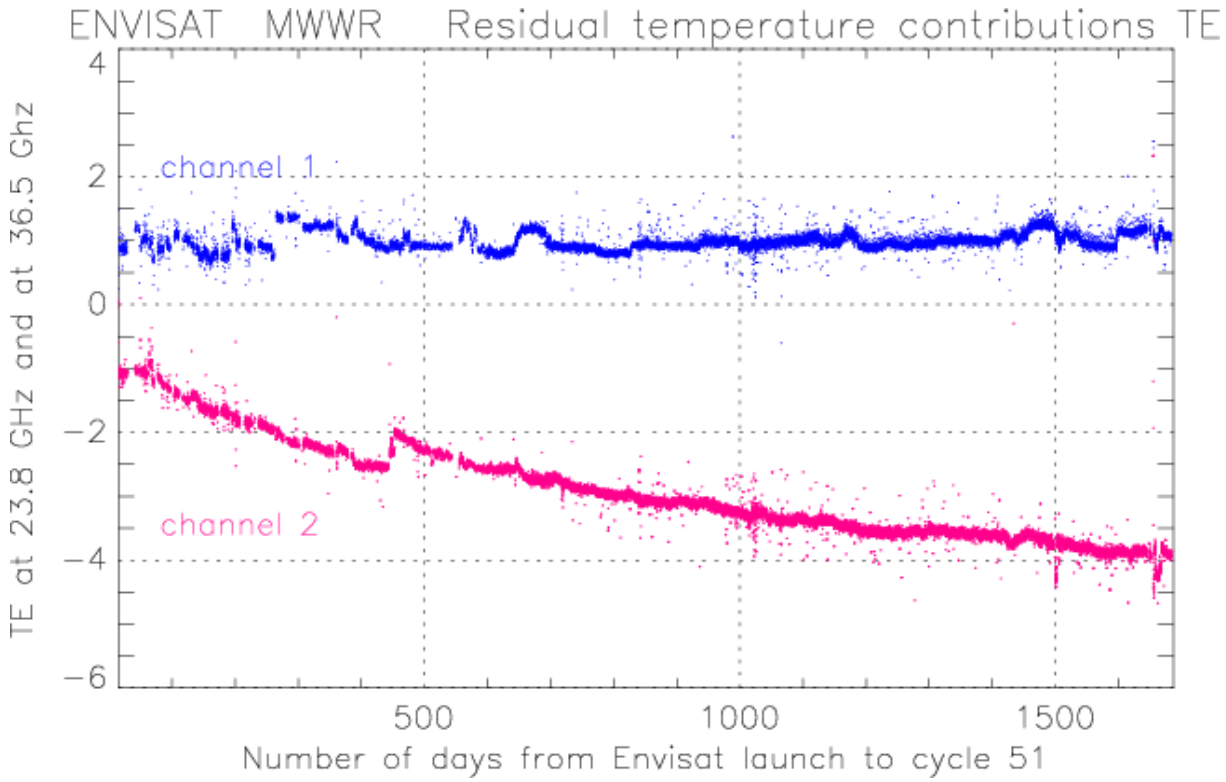

Figure 5: Time evolution of the residual temperature TE, since Envisat launch.

5 Monitoring of cold ocean brightness temperatures

To assess the long term stability of the ERS2 radiometer, monitoring of the two brightness temperatures was performed on several continental areas (Antarctic Plateau, South Greenland plateau, Amazon forest and Sahara desert) and by selecting the coldest measurements over ocean.
The latter method, derived from Ruf's one for TMR (Ruf, 2000), was found to be the most efficient to point out the slight trend of ERS2 channel A (Eymard et Obligis, 1999; Eymard et al, 2002).
The method consists of first filtering out data with value higher than a given threshold, then filtering out again the remaining data with values above the cycle average minus 1.5 times the standard deviation. Validation of the method was performed by checking its consistency on TMR data (in comparison with Ruf's results).
Following this method developed for the long-term monitoring of ERS2 and using a threshold equal to the average minus the standard deviation, the Envisat resulting time series is plotted in **figure 6**. For the first channel, the cold ocean TB values present a 0.0146 K/year variation, while a variation of 0.131 K/year is observed for the second one.

Note that a spike is observed around day 1300 (cycle 041) for both channels.

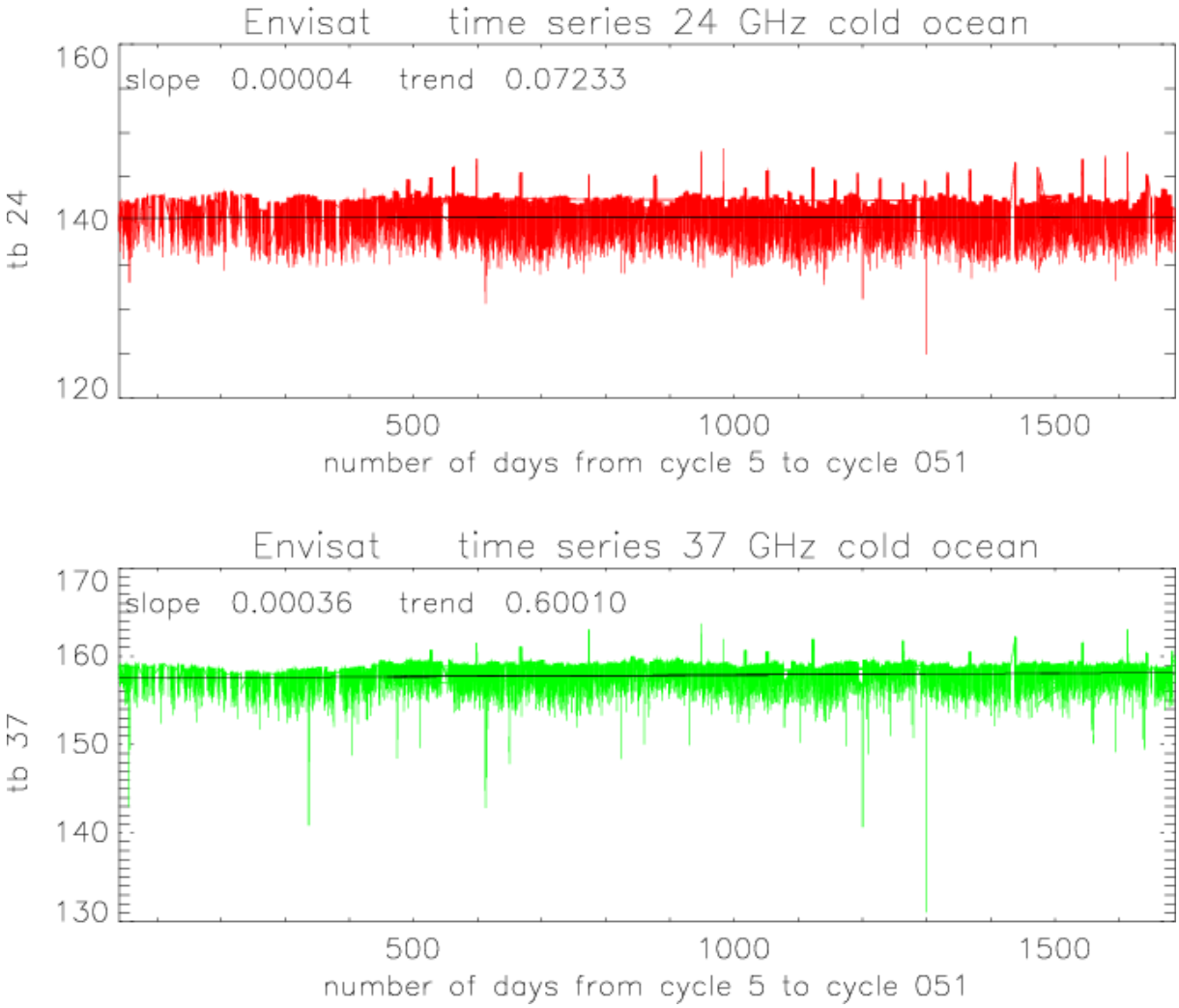

Figure 6: time series of the coldest brightness temperatures over ocean. The x-axis represents the number of days since Envisat launch. The data available before cycle 5 (corresponding to about 30 days) are not used for this monitoring

6 Conclusion on the cycle assessment and long term monitoring

The monitoring of the main instrumental parameters of the radiometer up to cycle 051 shows a drift of the 36.5 GHz channel. It appears that the gain, the sky horn counts, and the hot load counts have decreased between 3 and 19.92% since launch.
A big spike is also observed around day 1433 (cycle 044) for 23.8 GHz and 36.5 GHz channels.
A platform incident has occured during cycle 046, between day 1497 and day 1500 from launch.

The residual temperature is now 3.50 times higher in absolute value than the one estimated at the beginning of the mission and 4-6 times higher than the one expected from ground testing. No explanation is provided to date.
These features should impact the 36.5 GHz brightness temperature as reported in (Obligis et al, 2003). But as seen in the monitoring of the cold ocean brightness temperatures through the different previous reports the slope of the derived regression line varies at each cycle which makes the quantification of the real impact difficult since the variation observed on the cold TB is a combination of the instrumental features and the annual natural cycle.
Updated status on the 36.5 GHz channel drift was performed in April 2005 from 2 years of data (Tran et al, 2005) corresponding to the period from cycle 11 to cycle 31. This assessment pointed out an impact on 36.5 GHz brightness temperatures of about +0.5 K/year for TB at 150 K (synthesis from different methods at the low end of the TB histogram) and of +0.9 K/year at 250 K (synthesis from different methods at the high end of the TB histogram). Transcription of these results in term of effect on wet tropospheric path delay showed a decrease of about -0.9 mm/year at 5 cm (dry atmosphere) and -0.6 mm/year at 30 cm (wet atmosphere). This leads to observe significant impact on the global sea level rise estimation.
Moreover, the drift characteristics induce geographical errors, we observe systematic overestimation of sea level for dry atmospheres (high latitudes) (Obligis et al, 2005).

The table below sums up main monitoring anomalies observed since ENVISAT cycle 36 :

Cycle Number	Date since launch	Impacted Monitoring parameters
36	around 1150	Gain values and sky horn counts step down for 36.5 GHz channel.
41	around 1300	Spike on cold ocean TB values for both channels.
44	around 1433	Big spike on gain and TE values for both channels.
46	around 1500	Gain loss, sky horn counts and hot load counts spikes for both channels.
51	around 1650	Two unavailable L0 MWR data periods.

Table 1 : Main monitoring anomalies observed from cycle 36

7 Reference documents

Bernard et al, The microwave radiometer aboard ERS-1: Part 1 - characteristics and performances, IEEE Trans. Geosci. Remote Sensing, 31(6), 1186-1198, 1993.

Eymard et al, Intercomparison of TMR and ERS/MWR calibrations and drifts, SWT TOPEX-JASON, New Orleans, Oct. 2002.

Eymard et al, Reports on activities performed in 2001 on the ERS2/MWR survey, May 2002.

Eymard et Obligis, Preliminary report on long-term stability of ERS2/MWR over continental areas, 1999.

Obligis et al, An assessment of ENVISAT/MWR measurements and products, Envisat QWG meeting, 26-27 September 2005, Toulouse, France.

Obligis et al, Envisat/MWR: 36.5 GHz channel drift status, March 2003.

Ruf, Detection of calibration drifts in spaceborne microwave radiometers using a vicarious cold reference, IEEE Trans. Geosci. Remote Sens., 38(1), 44-52, 2000.

Tran, Obligis, and Eymard, Evaluation of Envisat MWR 36.5 GHz (updated status), CLS-DOS-NT-05-073 Report, 20 April 2005.